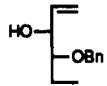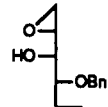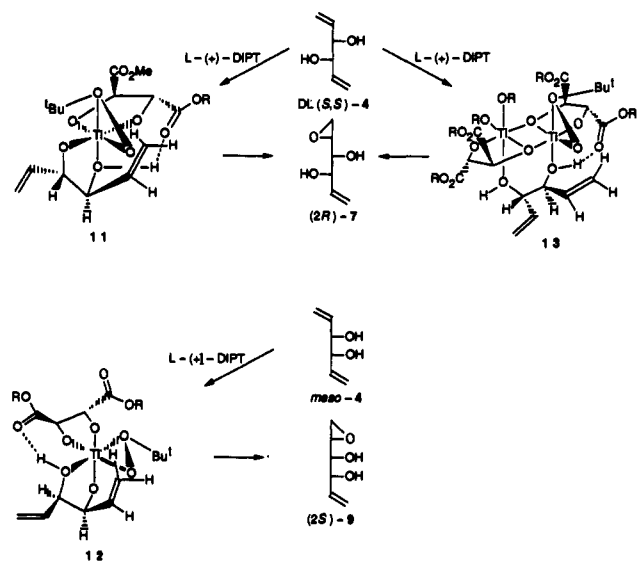**Table I.** Katsuki–Sharpless Asymmetric Epoxidation of 1,2-Divinylethylene Glycols

entry	substrate	catalyst (equiv) Ti/tartrate[a]	TBHP	time, h	product, %[c] (corrected yield)	opt. yield, % ee
1	DL-(R,R)-4	1.0/1.2[a,d]	1.2	10	(2S)-7, 32 (42)	~100[e]
					(2S,5S)-8, 19 (25)	~100[e]
2	DL-(R,R)-4	1.0/1.2[a]	3.0	20	(2S)-7, 9 (10)	~100[e]
					(2S,5S)-8, 35 (40)	~100[e]
3	DL-(±)-4	1.0/2.0[b]	2.0	10	(R,R)-4, 47	~83[f]
					(2R)-7, 11	~100[h]
					(2R,5R)-8, 6	~100[h]
4	DL-(±)-4	1.0/2.0[b]	10	8	(R,R)-4, 36	~88[f]
					(2R)-7, 3	~100[h]
					(2R,5R)-8, 12	~100[h]
5	(structure: HO— / —OBn)	1.0/1.2[b,g]	5	12	(structure: O / HO— / —OBn)	~100[e]
6	meso-4	0.4/0.8[b]	10	114	9, 28 (60)	~90[h]
					10, 4 (9)	~90[h]
7	meso-4	1.0/2.0[b]	10	72	9, 45 (53)	~90[h]
					10, 6 (8)	~90[h]
8	meso-4	1.0/2.0[b]	30	90	9, 57 (71)	~90[h]
					10, 7 (10)	~90[h]
					60 (82)	

[a] D-(–)-DIPT. [b] L-(+)-DIPT. [c] Due to water solubility, the oxidation products could not be isolated completely from the reaction mixture. Corrected yields were estimated on the basis of consumed starting material. [d] Reaction did not take place with L-(+)-DIPT. [e] Estimated by ^{1}H NMR analysis (500 MHz). [f] Estimated by specific rotations. [g] Reaction did not take place with D-(–)-DIPT. [h] Estimated by ^{1}H NMR analysis (500 MHz) of MTPA esters.

Scheme III

their stereochemistry unambiguously.

To explain the unexpected stereochemical outcome encountered in the Katsuki–Sharpless asymmetric epoxidation of both DL and meso substrates, we assume involvement of the hexacoordinated complexes, 11 for DL-4 and 12 for meso-14. In both of these, a near perpendicular alignment of the olefin axis and the epoxy chelate ring plane[14,15] may be preserved, leading to the corresponding epoxides in a stereospecific manner. Although the involvement of a dimeric complex,[2c,16] such as 13, may also account for the stereochemical outcome observed in the DL substrate, a similar dimeric complex having the optimal stereoelectronic arrangement leading to (2S)-7 seems unlikely from the meso

counterpart (meso-4) (Scheme III).

Supplementary Material Available: Schemes depicting various syntheses starting from (2S)-7, L-(+)-diethyl tartrate, (2S,5S)-8, D-mannitol, 9, and 10 (2 pages). Ordering information is given on any current masthead page.

Improving Two-Dimensional ^{1}H NMR NOESY Spectra of a Large Protein by Selective Deuteriation

Joseph Reisman,[†] Isabelle Jariel-Encontre,[‡] Victor L. Hsu,[†,§]
Joseph Parello,[‡] E. Peter Geiduschek,[∥] and
David R. Kearns*,[†]

*Department of Chemistry and Department of Biology
University of California, San Diego
9500 Gilman Drive, La Jolla, California 92093-0342
Unité de Recherche Associée au CNRS, No. 1111
Faculté de Pharmacie, 15 avenue Charles Flahault
34060 Montpellier-Cédex, France*

The accurate determination of interproton distances, as obtained from 2D nuclear Overhauser effect experiments (NOESY), is of primary importance in the determination of solution-state protein structures by NMR, while 2D J-correlated experiments (COSY) are crucial for the assignment of specific spin-system resonances.[1–3]

(13) Takano, S.; Iwabuchi, Y.; Ogasawara, K. *J. Chem. Soc., Chem. Commun.* **1989**, 1371–1372.
(14) Cf.: Corey, E. J. *J. Org. Chem.* **1990**, 55, 1693–1694.
(15) For brevity, L-(+)-tartrate is used as chiral catalyst in Scheme III.
(16) We thank one of referees for suggesting this complex.

[†] Department of Chemistry, University of California, San Diego.
[‡] Unité de Recherche Associée au CNRS.
[§] Present address: Department of Molecular Biophysics and Biochemistry, Yale University, New Haven, CT 06510.
[∥] Department of Biology, University of California, San Diego.
(1) Wüthrich, K. *NMR of Proteins and Nucleic Acids*; Wiley: New York, 1986.
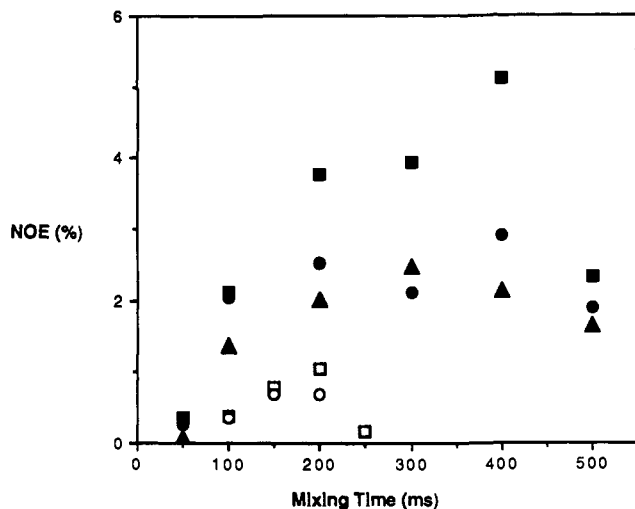(2) Wüthrich, K. *Methods Enzymol.* **1989**, 177, 125–131.

Figure 1. NOE buildup in the 500-MHz ^{1}H NOESY spectra of fully protiated and selectively deuteriated TF1. Intraresidue NOE buildups for phenylalanine 97 (□) ortho-α (7.33 × 4.49 ppm downfield of internal TMSP-d4), (○) ortho-β (7.33 × 3.16 ppm), and (△) ortho-β' (7.33 × 2.58 ppm) displayed as plots of percent NOE versus the mixing time, τ_m, for TF1-^{2}H[FGIY] (closed symbols) and for TF1-^{1}H (open symbols). Notice that the ortho-β' cross peak is not observed for TF1-^{1}H. Solution compositions: >99% ^{2}H$_2$O; NaCl, 50 mM; phosphate buffer, 50 mM, pH 7.0; aprotinin (as a protease inhibitor), 2 μM; TF1 dimer, 1.1 mM (TF1-^{1}H) or 1.5 mM (TF1-^{2}H[FGIY]), 30 °C. GE500 spectrometer settings: 90° pulse, 12 μs; recycle delay, 2 s; spectral window, 6024 Hz; 64 scans per t_1 value; 256 t_1 values. Time domain data were multiplied by a shifted (2.56°) sine bell in the t_2 dimension, Fourier transformed, transposed, multiplied by a shifted (5.12°) sine bell and zero-filled twice in the t_1 dimension, Fourier transformed, and displayed as absolute value intensities in a 1K × 1K real 2D frequency domain matrix. NOE intensities are expressed as a fraction of the Phe97 ortho diagonal-peak volume at zero τ_m (M_0) after normalization for a two-spin ortho site.[13] M_0 was derived by plotting the sum of diagonal-peak and all cross-peak volume integrals (for F_1 = 7.33 ppm) of the TF1-^{2}H[FGIY] sample as a function of τ_m and fitting to a single exponential. The derived initial magnetization, M_0, and the concentration ratio of the two samples were used to normalize the NOE buildup curves. Owing to the proximity of Phe97 ortho and para resonances (7.33 ppm and 7.36 ppm, respectively), the NOE values are likely to be somewhat underestimated.

The 2D ^{1}H NMR spectra of large proteins are characterized by cross-peak degeneracies and severe line broadening, making the assignment of individual cross peaks problematic. COSY spectra suffer from decreased sensitivity due to the large line widths associated with increased molecular weight. NOESY spectra are made more complex by the increased number of protons available for cross relaxation, as well as by the occurrence of spin-diffusion effects in large proteins.[4,5]

In our studies of transcription factor 1 (TF1, 23 kDa as a dimer) from *Bacillus subtilis* phage SPO1, we have devised a NOESY-dependent strategy employing selectively deuteriated protein variants—generally referred to as TF1-^{2}H[AA$_i$]—in which a few amino acid types (AA$_i$ for i < 5) appear in the protiated form and the remainder are deuteriated to a high level. Details of the production of such variants will be presented elsewhere. Here we present the initial analysis of 2D NOESY spectra for the selectively deuteriated variant of TF1 with protiated Phe, Gly, Ile, and Tyr (TF1-^{2}H[FGIY]) residues, establishing the advantage of using NOESY, rather than COSY, spectra for assigning spin systems. Without proximal protiated amino acids, intraresidue ^{1}H–^{1}H dipolar couplings will dominate the relaxation while in-

(3) Clore, G. M.; Gronenborn, A. M. *Crit. Rev. Biochem. Mol. Biol.* **1989**, *24*, 479–564.

(4) Neuhaus, D.; Williamson, M. *The Nuclear Overhauser Effect in Structural and Conformational Analysis*; VCH Publishers, Inc.: New York, 1989.

(5) For an explicit relation between spin diffusion, cross relaxation, and the correlation factor, $\omega\tau_c$, see: Krishnan, V. V.; Murali, N.; Kumar, A. *J. Magn. Reson.* **1989**, *84*, 255–267.
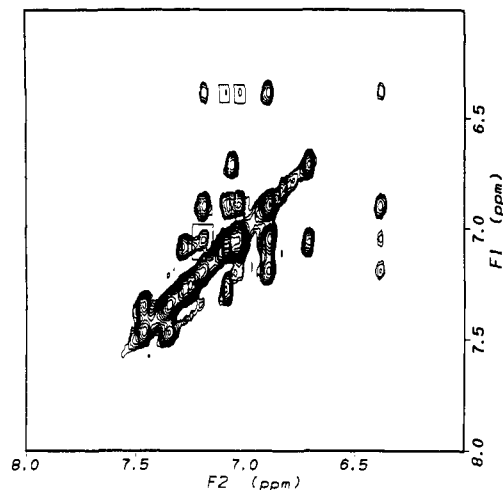
Figure 2. Contour plot of the aromatic region from a NOESY spectrum (τ_m = 400 ms) of TF1-^{2}H[FGIY]. Three interresidue cross peaks are highlighted: at 6.39 × 7.11 ppm, the Phe28 para-Phe47 para connectivity; at 6.39 × 7.03 ppm, the Phe28 para-Phe47 meta connectivity; and at 7.19 × 7.03 ppm, the Phe28 ortho-Phe47 meta connectivity. The interresidue cross peak Phe28 para-ortho appears at 6.39 × 7.19 ppm (see text). Sample conditions as in Figure 1. Spectrometer settings: 90° pulse, 12 μs; recycle delay, 1 s; spectral window, 6024 Hz; 160 scans per t_1 value; 256 t_1 values. Time domain data were multiplied by a shifted (60°) sine bell and zero-filled to 2048 real data points, Fourier transformed, transposed, multiplied by a shifted (60°) sine bell and zero-filled three times in the t_1 dimension, Fourier transformed, and displayed as phase-sensitive intensities in a 2K × 2K real 2D matrix.

terresidue pathways, contributing to additional spin diffusion, will be negligible. It is to be expected that NOE measurements will be favorably affected, yielding sufficiently larger intensities for specific cross peaks. In Figure 1, a comparison of Phe97 NOE buildup rates in TF1-^{1}H and TF1-^{2}H[FGIY], the selectivity deuteriated variant is characterized by larger NOE intensities through mixing times (τ_m) of 500 ms while the fully protiated TF1 displays weaker, earlier decaying cross-peak intensities due to the increased number of cross-relaxation pathways, the shorter proton relaxation times, and the associated spin-diffusion effects. A theoretical fitting of the buildup data would require a detailed TF1 structure. The relative intensities of the ortho-α and ortho-β cross peaks suggest a preferred side-chain orientation that could not be inferred from the TF1-^{1}H data.

As expected, T_1 measurements for the aromatic protons of TF1-^{1}H and TF1-^{2}H[FGIY] show that selective deuteriation increases all longitudinal relaxation times. However, only moderate nonselective T_1 enhancements (between 1.3 and 2.1) are observed, since all the intraresidue ^{1}H–^{1}H contacts are conserved for a given amino acid while only the effects of interresidue contacts are suppressed. The suppression of the latter improves the NOE measurements by making fewer cross-relaxation pathways available and by lengthening the T_1 values. Nevertheless, intraresidue cross relaxation is still present and facilitates identifying the spin system of a given residue through its NOE connectivities, replacing the less sensitive J-correlated experiments. This is the case for the aromatic residues of TF1-2H[FGIY], for which we observe second-order NOE buildup for Phe28 para-ortho, as well as meta-α, β, and β' connectivities (not shown). These second-order NOE connectivities have proven to be useful in the identification of all four phenylalanine spin systems in TF1 (to be published). Although a selectively deuteriated variant considerably restricts the number of interproton contacts between residues, several interresidue connectivities are still observable in TF1-^{2}H[FGIY]. Figure 2 displays highlighted interresidue cross peaks between the aromatic protons of Phe28 and Phe47 at τ_m = 400 ms. Connectivities between the aromatic protons of Phe61 and Phe97 at τ_m = 600 ms (data not shown) are also seen.[6] Such

(6) Sequence-specific assignments are derived from the NOESY analysis of selected deuteriated TF1 variants and of TF1 mutants.

sequentially distant contacts are crucial in determining the folding of the TF1 dimer. Modeling studies based on the partially homologous *Bacillus stearothermophilus* HU protein[7] suggest that these are intermonomeric contacts. These contacts are not seen in similar experiments for TF1-[1]H.

The selective deuteriation approach reported here should simplify the identification of spin systems in large proteins by using a complementary set of deuteriated protein variants. The NOESY spectra of TF1-[2]H[FGIY] can be more accurately analyzed than those of the normally protiated protein. Spin-system identification in the TF1 23-kDa dimer (work in progress) relies more on NOE- than *J*-derived connectivities, as in a recently published study of the *Escherichia coli* trp repressor, a 25-kDa dimer.[8]

In closing, we mention that the use of biosynthetically deuteriated proteins for NMR studies has a long history.[9] However, it is only recently through 2D correlated ^{1}H NMR spectroscopy that the benefits of deuteriation for larger proteins may be fully appraised.[10,11] The use of selectivity deuteriated amino acids, instead of the fully protiated amino acids used here, as well as the use of homonuclear 3D NMR methods,[12] should increase the potential of our proposed strategy.

(7) White, S. W.; Appelt, K.; Wilson, K. S.; Tanaka, I. *Proteins: Struct., Funct., Genet.* **1989**, *5*, 281–288. White, S. W., personal communication.

(8) Arrowsmith, C. H.; Pachter, R.; Altman, R. B.; Iyer, S. B.; Jardetzky, O. *Biochemistry* **1990**, *29*, 6332–6341.

(9) For a recent review, see: LeMaster, D. M. *Q. Rev. Biophys.* **1990**, *23*, 133–173.

(10) Torchia, D. A.; Sparks, S. W.; Bax, A. *J. Am. Chem. Soc.* **1988**, *110*, 2320–2321.

(11) LeMaster, D. M.; Richards, F. M. *Biochemistry* **1988**, *27*, 142–150.

(12) Padilla, A.; Vuister, G. W.; Boelens, R.; Kleywegt, G. J.; Cavé, A.; Parello, J.; Kaptein, R. *J. Am. Chem. Soc.* **1990**, *112*, 5024–5030 and references therein.

(13) Yip, P. F. *J. Magn. Reson.* **1990**, *90*, 382–383.

Total Synthesis of the Dibenzopyrrocoline Alkaloid (S)-(+)-Cryptaustoline. Revision of Absolute Configuration Due to an Unusual Inversion in Stereochemistry

A. I. Meyers* and Thais M. Sielecki

Department of Chemistry, Colorado State University
Fort Collins, Colorado 80523

Received November 8, 1990

During studies designed to show further synthetic applications of chiral formamidines toward enantiomerically pure isoquinoline alkaloids,[1] we targeted (−)-cryptaustoline (**1a**) as a suitable goal. The latter, isolated in 1952[2] from *Cryptocarya bowiei* (Hook) Druce indigenous to Queensland, Australia, was one of only two dibenzopyrrocoline alkaloids obtained from this substance, the other being cryptowoline (**2a**). Stereochemical assignments and

(−)-**1a**, R = Me, R[1] = H
(−)-**1b**, R = R[1] = H

(−)-**2a**
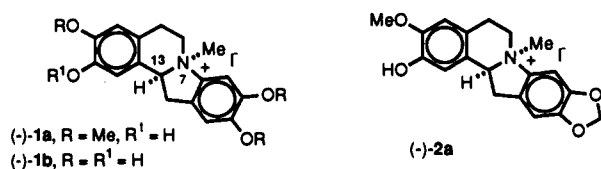
(1) For recent representative illustrations of this methodology, see: (a) Meyers, A. I.; Guiles, J. *Heterocycles* **1989**, *28*, 295. (b) Meyers, A. I.; Bös, M.; Dickman, D. A. *Tetrahedron* **1987**, *43*, 5095. (c) Meyers, A. I.; Gottlieb, L. *J. Org. Chem.* **1990**, *55*, 5659.

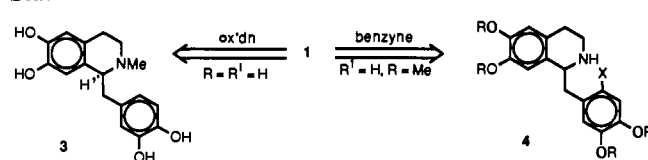(2) Ewing, J.; Hughes, G.; Ritchie, E.; Taylor, W. C. *Nature* **1952**, *169*, 618.

Scheme I

Table I. Cotton Effect of Intermediates[a]

formamidine route		oxidative coupling route[b]	
compd	λ, nm (ΔE)	compd[c]	λ, nm (ΔE)
(+)-**6**	286 (+1.58)	(+)-**3**	298 (+1.67)
(+)-**7**	286 (+0.97)	(−)-**1** (R = H)	298 (−0.94)
(+)-**1a**	290 (+1.45)	(−)-**1** (R = Me)	293 (−1.18)

[a] Taken in 95% ethanol. [b] References 3 and 7. [c] Refers to compounds in Scheme I.

total synthesis of **1** were reported by the Australian Group,[2,3] two Japanese groups,[4,5] and two American groups.[6,7] Interestingly, the alkaloidal system was predicted by Robinson[8] and Schopf[9] in 1932 when they observed a facile ring closure of the racemic 1-benzylisoquinoline **3** upon treatment with oxidizing agents to give the benzopyrrocolines **1** or **2**. Many years later both Ewing et al.[3] and Brossi[7] showed that **3** can be transformed into the alkaloid by oxidative coupling using chloranil or horseradish peroxidase, respectively, and also reported that the absolute configuration of **1** was *S* at C-13. These assignments were based on completely sound conclusions since both laboratories began by using (+)-**3** with known absolute configuration and arrived at **1** with high optical activity and "complete retention of configuration" at C-13. Furthermore, a more recent study confirmed that the *N*-methyl group in **1** was cis to the C-13 proton using NOE techniques.[5b] Another approach to the benzopyrrocoline system **1** is the use of a benzyne precursor,[10,11] **4** (X = Cl, Br), which, when treated with a strong base, leads to the benzyne and undergoes an intramolecular addition by the amino group. Satisfied that the structure and stereochemistry of cryptaustoline **1a** was on firm ground, we embarked on a synthetic route to produce the "natural enantiomer *S*-(+)", in an asymmetric manner.[1]

Transformation of **6**, prepared as described previously,[1] into the tetracyclic system **7** was readily accomplished by treating a solution in THF at −100 °C with 2.1 equiv of *n*-butyllithium. Following chromatography (silica gel, EtOAc–hexane–Et₃N, 3:6:1), (+)-**7** was obtained as a crystalline product [mp 131–132 °C (lit.[10] mp 126–128 °C); [α]D +48.5° (c 1.0, acetone)]. Methyl iodide was introduced to form the *N*-methyl quaternary salt [mp 224 °C (lit.[10] mp 224–226 °C)], and then debenzylation was performed (benzene, concentrated HCl, KI, 50 °C, 3 h) to furnish cryptaustoline **1a** [mp 256–258 °C dec (lit. racemate[10,2] mp 258–260 °C dec)]. The specific rotation observed, however, was [α]D +141° (c 0.2, EtOH), which was *opposite in sign* to the purported *S*-(−) natural product ([α]D = −150°). On the basis of the magnitude of the rotation, the asymmetric synthesis was performed in 94% ee. Since the formamidine methodology has consistently afforded *S*-1-substituted tetrahydroisoquinolines,[1] the

(3) Hughes, G. K.; Ritchie, E.; Taylor, W. C. *Aust. J. Chem.* **1953**, *6*, 315.

(4) Yasuda, S.; Hirasawa, T.; Yoshida, S.; Hanaoka, M. *Chem. Pharm. Bull.* **1989**, *37*, 1682.

(5) (a) Takano, S.; Satoh, S.; Ogasawara, K. *Heterocycles* **1987**, *26*, 1483. (b) Takano, S.; Satoh, S.; Oshima, Y.; Ogasawara, K. *Heterocycles* **1987**, *26*, 1487.

(6) Benington, F.; Morin, R. D. *J. Org. Chem.* **1967**, *32*, 1050.

(7) Brossi, A.; Ramel, A.; O'Brien, J.; Tietel, S. *Chem. Pharm. Bull.* **1973**, *8*, 1839.

(8) Robinson, R.; Sugasawa, S. *J. Chem. Soc.* **1932**, 789.

(9) Schopf, C.; Thierfelder, K. *Justus Liebigs Ann. Chem.* **1932**, *498*, 22.

(10) Kametani, T.; Ogasawara, K. *J. Chem. Soc. C* **1967**, 2208.

(11) However, strong bases have been reported to racemize 1-substituted isoquinolines: Brossi, A.; Rahman, M.; Rice, K.; Gehrig, M.; Borer, R.; O'Brien, J.; Tietel, S. *Heterocycles* **1977**, *7*, 277. Teitel, S.; O'Brien, J. *J. Org. Chem.* **1976**, *41*, 1657.